THE NATURE OF SILICON-OXYGEN BONDS IN SILICA POLYMORPHS

B. SILVI, A. SAVIN AND F. R. WAGNER*
Laboratoire de Chimie Théorique,
Université Pierre et Marie Curie,
4, Place Jussieu, 75232 Paris cedex (France)
* *present address: Institut für Anorganische und Analytische Chemie und Radiochemie,*
Universität des Saarlandes Im Stadtwald,
66123 Saarbrücken (Germany)

1. Introduction

Quantum chemists have devoted considerable effort in order to understand the nature of the chemical bond in silicated minerals. The pioneering work of Linus Pauling[1, 2, 3] provides a first example in which the valence bond concept is used in order to explain why the SiO bond length in silicates is less than the sum of the single bond radii of the two atoms. Moreover, this interpretation emphasizes the role of $3d$ orbitals through a sp^3d^2 hybridization of the silicon. With the advent of efficient computational facilities and of molecular *ab initio* softwares, several leading groups have published reliable calculations performed within the cluster, or more precisely prototype molecule framework. Information provided by such calculations concern several important domains. Born-Oppenheimer energy surfaces allow to set up site-site or covalent potentials to be used in further lattice dynamics or molecular dynamics studies. Important advances in this area are due to Gibbs *et al*[4], Lasaga *et al*[5], Tsuneyuki *et al*[6] and Kramers *et al*[7]. Interaction of such prototype silicated molecules with other reactant molecules, such as water or ammonia, allows to model the catalytic properties of zeolite[8, 9, 10]. Finally, the study of the electronic structure is of primary importance for understanding the bonding. One important result of the earlier *ab initio* calculations was to discard the possible contribution of silicon d orbitals to the bonding. Most calculations on prototype

B. Silvi and P. D'Arco (eds.), Modelling of Minerals and Silicated Materials, 179–199.

on prototype molecules performed either with minimal or split valence basis sets[11], as well as periodic Hartree-Fock calculations of quartz[12, 13], cristobalite and tridymite[12, 14] correctly reproduce the experimental Si-O bond length. Improvement brought by $3d$ function is less important in this respect and are of the order of what is expected from polarization functions. G. V. Gibbs and his team have been continuously concerned by the understanding of the nature of the SiO bond. They started their analysis with the available quantum chemical tools such as the Mulliken population analysis and electron density difference maps. However, they rapidly realized the limitations of these techniques which rely too much upon the approximations made in the actual calculations of electronic structures. A better "trail toward the Grail"[15] is provided by the theory of Atoms in Molecules of Richard Bader[16]. In a chapter of the present book, Gibbs *et al* discuss in details the limitations of electron density difference maps and show how efficient Bader's analysis is. However, the information carried by the electron density alone is not sufficient to clearly characterize the nature of the bonds. In a recent paper[17], we have shown that the topological analysis of a local function, which is related to the local kinetic energy excess due to the Pauli repulsion, can be used to characterize and define chemical bonds. The topological analysis of the so-called electron localization function (ELF), originally proposed by Becke and Edgecombe[18], provides a set of mathematizable definitions of the bond type.

In this chapter, the main lines of this new theory of chemical bond are presented in details and then it is applied to representative tetracoordinated and hexacoordinated silica polymorphs, namely low quartz, low cristobalite stishovite, the recently discovered $CaCl_2$-like high pressure phase and a prototype fluorite structure in which silicons are octacoordinated.

2. The topological classification of chemical bonds

The conventional tools used in Quantum Chemistry to characterize the bonding (population analysis, orbital localization) mostly rely on concepts related to the approximate treatment of many electron systems such as orbitals, valence-bond structures, atomic basis. In their spirit, they give an illegitimate physical content to mathematical objects which appear as intermediates along the calculation. This transgression of the interpretative postulates of Quantum Mechanics is done in order to conciliate the "atoms in molecules" and localized bonds of the chemical common sense with the impossibility of partitioning the molecular hamiltonian into atomic and bonding contributions. Their reliability is very questionable and results are highly method dependent. Moreover, these methods only apply in a LCAO framework and therefore are useless for calculations performed within plane-wave basis functions, one-center expansions, numerical functions, quantum Monte Carlo and correlated basis function frameworks. The necessary information cannot be extracted neither from experiment nor from an exact wavefunction.

In order to design a more rigorous theory of chemical bonds consistent with both Quantum Mechanics and chemical experience it is necessary to invoke an external mathematical theory able to extract qualitative information from quantitative. The topological analysis of the gradient vector field of a local function which carries the physical information is the well-established mathematical approach to handle this problem[19].

2.1. KINETIC ENERGY RELATED LOCAL FUNCTIONS

The formation of a chemical bond from fragments is the result of a competition between the potential and kinetic energies which leads to an optimal lowering of the total energy. As pointed out by Ruedenberg[20] : "Delocalization of the valence electrons from one atom to several atoms leads to a lowering of the kinetic energy pressure and, as a consequence there results a firmer attachment of these electrons to the nuclei with a concomitant lowering of the total energy." The importance of the kinetic energy contribution to the bonding is specifically a quantum effect which can be interpreted as a consequence of the uncertainty principle[20]. Once again, we will quote Ruedenberg who states :"The wave mechanical kinetic behavior, which differs typically from the classical behavior and is characterized by the cue *uncertainty principle,* is a fundamentally essential element of covalent binding. Any explanation of chemical binding based essentially on electrostatics, or any other nonkinetic concept, misses the very reason why quantum mechanics can explain chemical binding, whereas classical mechanics cannot".

The study of the chemical bond from a local kinetic energy point of view, is therefore expected to bring a deeper insight into the understanding of its nature. For this purpose we need to calculate and to analyze the one particle kinetic energy density. In principle, this function, $K(\mathbf{r})$ should be calculated from its classical analog :

$$K(\mathbf{r}) = \int F(\mathbf{r},\mathbf{p})(\frac{\mathbf{p}^2}{2m})d\mathbf{p} \qquad (1)$$

in which, m is the mass of the particle and $F(\mathbf{r},\mathbf{p})$ stands for the joint distribution of position and momentum. Unfortunately, a true joint distribution cannot be defined in Quantum Mechanics. It is nevertheless possible to introduce the so-called phase-space quasi distributions, such as the Wigner function, in order to get an expression which has the property when integrated over all space, yields the proper expectation value of the kinetic

energy. The quasi distributions are build up from correspondence rules and are required to yield the correct marginal distributions. As discussed by Shewell[21], the joint operators derived from the correspondence rules may not fulfill the requirement of uniqueness (i.e different operators for one physical quantity) or yield results in contradiction with the current interpretation of quantum mechanics. Moreover, there is no reason to use one rule rather than another. Cohen has shown[22] that all the possible phase-space distribution functions which obey the correspondence rules and yield correct marginal distributions belong to a given class of analytical functions of the form :

$$F(\mathbf{r},\mathbf{p}) = \left(\frac{1}{6}\right)^6 \int \exp[-\imath\tau\cdot\mathbf{p} + \imath\theta\cdot(\mathbf{u}-\mathbf{r})] f(\theta,\tau) \times \psi^*(\mathbf{u}-\frac{1}{2}\tau)\psi(\mathbf{u}+\frac{1}{2}\tau) d\theta d\tau d\mathbf{u} \quad (2)$$

where $f(\theta,\tau)$ is any function which satisfies

$$f(0,\tau) = f(\tau,0) = 1. \quad (3)$$

The relevance of quasi-distributions in physical applications has been discussed by Dahl [23] who has shown that the Wigner function is the only one which satisfies strong requirements such as being the expectation value of the so-called Wigner operator and therefore to be a description based on observables in the sense of Dirac [24]. For one particle, the corresponding possible form of the kinetic energy density is thus given by[25] :

$$K(\mathbf{r}) = \frac{1}{2}|\nabla\psi|^2 - \frac{1}{8}\nabla^2|\psi|^2 - \left(\frac{1}{2\pi}\right)^3 \int \exp[\imath\theta\cdot(\mathbf{u}-\mathbf{r})] \left\{\frac{|\psi(\mathbf{u})|^2}{2}\nabla_\tau^2 f(\theta,\tau)|_{\tau=0} + \imath\nabla_\tau f(\theta,\tau)|_{\tau=0}\cdot J(\mathbf{u})\right\} d\theta d\mathbf{u} \quad (4)$$

where J is the quantum mechanical current

$$J = \frac{\imath}{2}(\psi\nabla\psi^* - \psi^*\nabla\psi) \quad (5)$$

Generalization to a many particle system is straightforward.

$K(\mathbf{r})$ appears to be the sum of two contributions : the first one $T(\mathbf{r}) = \frac{1}{2}|\nabla\psi|^2$ yields the expectation value of the kinetic energy when integrated over all space. This contribution is always positive, it is called the definite positive kinetic energy density. The integral over space of the remaining contribution vanishes. For either a real wavefunction or a stationary state the quantum mechanical current is zero and therefore this remaining term

can be expressed in terms of the $f(\theta,\tau)$ function, of the density and of their derivatives.

For a quantum system with a given one particle density, $T(\mathbf{r})$ is the only term which is sensitive to the nature (fermion or boson) of the particles. For a many-fermion system, $T(\mathbf{r})$ can be formally expressed as the sum of two contributions, one of which accounting for the Pauli principle and the other not. However, another partition scheme in which the total kinetic energy is written as the sum of the von Weizsäcker term $T_W(\mathbf{r})$[26] and of a remaining non-von Weizsäcker term $T_{nW}(\mathbf{r})$ term has been generally adopted[27, 28, 29, 30]. The von Weizsäcker term :

$$T_W(\mathbf{r}) = \frac{1}{8}\frac{|\nabla\rho(\mathbf{r})|^2}{\rho(\mathbf{r})} \quad (6)$$

corresponds to the definite positive kinetic energy density of a system of independent particles with the density $\rho(\mathbf{r})$. The non-von Weizsäcker term includes the Coulomb and Fermi correlation contributions to the kinetic energy density, its expression involves therefore quantities related to the second order density matrix. Tal and Bader[27] have established that $T_{nW}(\mathbf{r})$ is a true lower bound to the definite positive kinetic energy density, i.e :

$$T_{nW}(\mathbf{r}) = \frac{1}{2}|\nabla\psi|^2 - \frac{1}{8}\frac{|\nabla\rho(\mathbf{r})|^2}{\rho(\mathbf{r})} \geq 0 \quad (7)$$

Moreover, this term is the difference of the kinetic energy density of the actual system and of that of a system of spin-free independent particles both with identical one-particle densities $\rho(\mathbf{r})$. For real wavefunctions or for stationary states, it is simply the difference of the definite positive kinetic energies since the (unwanted) remaining contributions cancel one another. Another attractive property of the non-von Weizsäcker contribution is that it appears to be the trace of the Fisher's Information matrix[28].

For practical applications, we will not consider $T(\mathbf{r})$ itself but rather the definite positive kinetic energy density of independent particles $T_s(\mathbf{r})$ which appears in the exact density functional theory[31]. Within this framework, the non-von Weizsäcker term accounts only for the Fermi correlation and is usually referred to as Pauli kinetic energy density[32]. Another propery of $T_{nW}(\mathbf{r})$ is its relationship to the conditional probability $P^{\sigma\sigma}_{cond}(\mathbf{r},\mathbf{r}')$ for electrons of parallel spin in the single determinental approximation :

$$T_{nW}(\mathbf{r}) = \nabla^2_{\mathbf{r}'} P^{\sigma\sigma}_{cond}(\mathbf{r},\mathbf{r}')\Big|_{\mathbf{r}'=\mathbf{r}} \quad (8)$$

In the original definition of ELF, given by Becke and Edgecombe [18], $P^{\sigma\sigma}_{cond}(\mathbf{r},\mathbf{r}')$ was used.

The definite positive kinetic energy density has received a considerable attention in order to build approximate kinetic energy functionals to be used in a density functional theory not based on orbitals (for a review of such functionals see Lacks and Gordon[33]). Among the most promising routes to this goal, we can mention the approximation proposed by Lee, Lee and Parr[34] :

$$T_s(\mathbf{r}) \approx C_F \rho^{5/3}(\mathbf{r}) F(s(\mathbf{r})) \tag{9}$$

in which $C_F = \frac{3}{10}(3\pi^2)^{2/3}$, $F(s(\mathbf{r}))$ is a function which accounts for the deviation from uniformity and homogeneity and $s(\mathbf{r})$ the scaled density gradient defined by :

$$s(\mathbf{r}) = \frac{|\nabla\rho(\mathbf{r})|}{2(3\pi^2)^{2/3}\rho^{4/3}(\mathbf{r})} \tag{10}$$

For slowly varying densities, the kinetic energy functional can be represented by one of its gradient expansions. The gradient expansion of the kinetic energy density is not unique since it relies upon different derivations techniques [35], which yield or not a contibution of the laplacian of the density in the second order correction. In the following we will consider the expansion expression which does not involve $\nabla^2\rho(\mathbf{r})$:

$$T_s(\mathbf{r}) = C_F\rho^{5/3}(\mathbf{r}) + \frac{1}{72}\frac{|\nabla\rho(\mathbf{r})|^2}{\rho(\mathbf{r})} + \ldots = C_F\rho^{5/3}(\mathbf{r})\left(1 + \frac{5}{27}s^2(\mathbf{r}) + \ldots\right) \tag{11}$$

A similar expression can be derived for the non-von Weizsäcker contribution :

$$T_{nW}(\mathbf{r}) = C_F\rho^{5/3}(\mathbf{r}) - \frac{1}{9}\frac{|\nabla\rho(\mathbf{r})|^2}{\rho(\mathbf{r})} + \ldots = C_F\rho^{5/3}(\mathbf{r})\left(1 - \frac{40}{27}s^2(\mathbf{r}) + \ldots\right) \tag{12}$$

The scaling by $\rho^{5/3}$ is made in order to minimize as well as possible the density dependence of the measure of the deviation from uniformity and homogeneity.

We consider now the class of parametrized local functions :

$$G(\mathbf{r};a) = C_F^{-1}\rho^{-5/3}\left(T_s(\mathbf{r}) - aT_W(\mathbf{r})\right) \tag{13}$$

in which the parameter a lies in the interval [0,1]. All these functions are positive. It is possible to make a transformation in order to confine them in the range [0,1], either with the scheme proposed by Becke and Edgecombe for ELF[18] :

$$\eta_a(\mathbf{r}) = \left(G(\mathbf{r};a)^2 + 1\right)^{-1} \tag{14}$$

or with :

$$\vartheta_a(\mathbf{r}) = \exp\left(-G(\mathbf{r};a)\right) \tag{15}$$

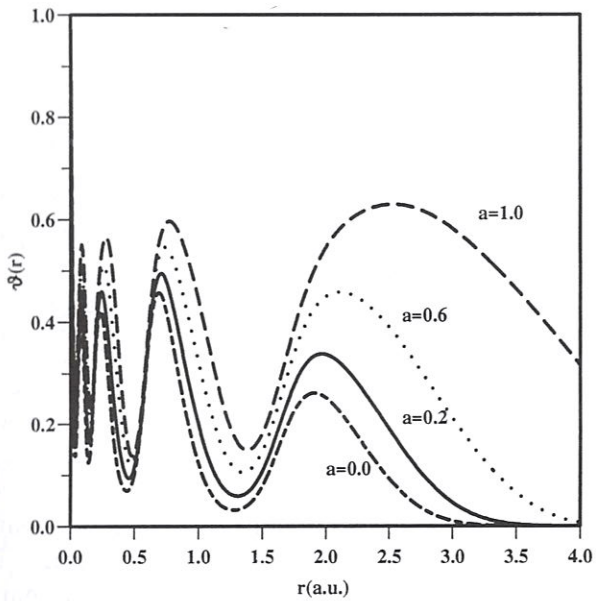

Figure 1. Radial localization functions $\vartheta_a(\mathbf{r})$ for xenon.

$\eta_1(\mathbf{r})$ is the original ELF function. For a given value of a both $\eta_a(\mathbf{r})$, $\vartheta_a(\mathbf{r})$ and $G(\mathbf{r};a)$ have their extrema at identical positions. These functions display the shell structure of atoms up to the O shell as shown for xenon on figure 1. The increase of the a parameter slightly shifts the locations of the maxima and minima of ϑ_a towards larger values of r. It is worthy to note, that in contrast with the usual orbital model there is no subshell structure, although the curves were generated from a Hartree-Fock wavefunction.

These functions provide a local measure of the effect of the Pauli repulsion on the kinetic energy density. In the region of space where the Pauli repulsion is weaker than in a uniform electron gas of identical density, we should say where the local parallel pairing is lower, $\eta_a(\mathbf{r})$ and $\vartheta_a(\mathbf{r})$ are respectively larger than 0.5 and 0.36. In the regions where the local parallel pairing is higher (and therefore the Pauli repulsion strongly active) they are lower than these latter values. Up to now, only η_1 (i.e. ELF) has been extensively used.

2.2. SKETCH OF THE TOPOLOGICAL ANALYSIS OF DYNAMICAL SYSTEMS

The topological analysis of local function provides a partition of the space, for our purpose the molecular space, which is analogous to the more familiar partition made in hydrology in river basins delimited by watersheds. In this

paragraph we intend to provide the definitions of the essential concepts for those of the readers who are not trained in this part of mathematics.

By definition a *dynamical system* is a field of bound vectors X on a manifold M. For each and every point of M of coordinates $\{m\}$ the equations $dm/dt = X(m)$ determine a unique trajectory $h(m)$. Although the analogy with a velocity field is purely formal, the method has been widely used to model the time evolution of many phenomena. The trajectories begin and end in the neighbourhood of points for which $X(m) = 0$. For a given point p belonging to M, $\alpha(p)$ and $\omega(p)$ denote the limit-sets of $p(t)$ in M corresponding respectively to $t \to \infty$ and to $t \to -\infty$.

A *gradient dynamical system* is a dynamical system for which the vector field X derives from a scalar function V, called the *potential* function, that is $X = \nabla V$. The word potential is here somehow confusing because it has not exactly the same meaning as in Mechanics where minus the gradient field of the potential energy is not the velocity field but the force field and therefore is proportional to the acceleration field. For a gradient dynamical system, the *critical points* (i.e those for which $\nabla V = 0$) are single points in the most general case. Exceptions may occur if the system belongs to a continuous symmetry group, in such case those critical points which are not located on the infinite order symmetry element form (in $\mathbb{R}^3$) either a sphere ($SO(3)$ group) or a circle (C_∞ group). A convenient choice of the coordinate system allows to exploit the symmetry in order to reduce the dimensions and to remove the degeneracy of the critical points.

The *stable manifold* or *inset* of a critical point is the set of all the points for which this critical point is an ω-limit, the *unstable manifold* or *outset* the set of those for which it is an α-limit. The critical points of a gradient dynamical system are classified according to the number of positive *critical exponents*, here the eigenvalues of the hessian matrix, the *index* which is also the dimension of its unstable manifold. The index of a critical point m of the vector field X is denoted by $I(X, m)$. They are also denoted by a pair of integers (r, s), the rank (number of non-zero eigenvalues) and the signature (number of positive minus negative eigenvalues) of the hessian matrix. In the euclidian 3-dimensional space, there are four kinds of critical points : the *repellors* of index 3, noted $(3, 3)$, which are the local minima of the potential function; the saddle points $(3, 1)$ and $(3, -1)$ of index respectively 2 and 1; the *attractors* (3, -3) of index 0 which are the local maxima of the potential function. Attractors are only ω-limits, repellors only α-limits whereas saddle points are both. The stable manifold of an attractor is called the *basin* of the attractor. The *separatrices* are the boundary points, lines or surfaces of two or more basins. They are the stable manifolds of the saddle points. The number of *hyperbolic* critical points (i.e. without zero critical exponent) satisfies the phase-rule type relationship which is given by the Poincaré-Hopf theorem :

$$\sum (-1)^{I(X,m)} = \chi(M) \tag{16}$$

The sum runs over the critical points of the vector field X bound on the manifold M and $\chi(M)$ is the Euler characteristic of the manifold. For finite and periodic systems in $\mathbb{R}^q$, $q \leq 3$, the Euler characteristic is 1 and 0 respectively.

Another very helpful concept is that of domain. Let M' a subset of the manifold M, if for any couple of points a and b there exists a path joining a and b totally contained in M' then M' is a domain. In the case of the gradient field analysis, volumes bounded by a given isosurface of the potential function form domains. For a given potential function the number of domains depends upon the value defining the isosurfaces. We have been led to consider two types of domains according to the number of attractors lying within them. A domain contains at least one attractor. In this case it is said to be irreducible because the increase of the value defining its bounding isosurface below the value of the potential function at the attractor cannot give rise a splitting into several new domains. If a domain contains more than one attractor, it is reducible because it is possible to get new domains by increasing the value of the bounding isosurface. The values of the bonding isosurface which correspond to domain separation are those taken by the potential function at the critical points located on the separatrix surface between two basins.

2.3. THE TOPOLOGICAL ANALYSIS OF ELF

The localization functions described previously are scalar functions the gradient field analysis of which allows to locate attractors and basins with a clear chemical signification[17]. Usually, the attractors of a gradient field are single points as it is the case for the gradient field of the density. However, for the ELF function, they can also be circles and spheres if the system belongs to a continuous symmetry group (here, cylindrical and spherical symmetry respectively).

2.3.1. *Classification of basins*

There are basically two types of basins. On the one hand are core basins organized around nuclei (with $Z > 2$) and on the other are valence basins in the remaining space. The structure provided by the core basins closely matches the inner atomic shell structure. A valence basin is characterized by its synaptic order which is the number of cores to which it is connected [36]. To be connected to a core a valence basin must fulfill the three following conditions :

i) It is bounded to the core basin by a part of a common separatrix.
ii) The valence attractor lies within the smallest (reducible or irreducible) valence f-localization domain which totally surrounds another f-localization domain which contains one or more core attractors.
iii) The proton is counted as a formal core.

In principle, a core is always totally encapsulated by at least one valence basin and therefore propositions i) and ii) are redundant when f tends to zero unless the valence localization domains and a core domain have already merged into a single domian. In our description of the chemical bond a basin which contains a proton is considered as a valence basin except for the peculiar case of the very strong hydrogen bond for which a pseudo core shell is found around the bridging proton. The valence basins are therefore divided into mono-, di- and polysynaptic ones. As an example, a C-H bond is characterized by a disynaptic basin which encompasses the proton and shares a common separatrix with the carbon core basin. The nomenclature adopted to label core and valence attractors and basins is given in table 1. The attractors and basins are labeled as $T_{[i]}$(atom labels). T denotes

TABLE 1. Nomenclature of attractors and basins.

synaptic order	nomenclature	symbol
0	core	$C(X_i)$
1	monosynaptic	$V(X_i)$
2	disynaptic	$V(X_i, Y_j)$
≥ 3	polysynaptic	$V(X_i, Y_j, \ldots)$

the type of attractor, V for valence, C for core ; i is an optional running number in the case of multiple attractors related to the same atom(s). For example, in the water molecule there is one core attractor for the oxygen K-shell labeled C(O), two protonated disynaptic attractors $V(H_1, O)$ and $V(H_2, O)$, and two monosynaptic attractors corresponding to the lone pairs $V_1(O)$ and $V_2(O)$. In ethane, the disynaptic attractor of the C-C bond will be named $V(C_1, C_2)$ accordingly.

The classification of bonds proposed previously remains valid with this new nomenclature. The shared electron interaction (a more consistent name is shared valence basin interaction) is characterized by a di or polysynaptic basin. The lone pairs give rise to monosynaptic basins. It is important to note that this picture of the chemical bond implies a somehow different point of view than that currently adopted in Chemistry. In the standard pictures a bond is considered as a link joining an atom to another one. Here, what is important is the number of cores a given piece of glue (the valence basin) is stuck on.

2.3.2. *The hierarchy of localization basins*
Another criterion of discrimination between basins is provided by the reduction of reducible domains. The reduction of a reducible localization domain occurs at a critical value of the bounding isosurface, over which the domain is split into domains containing fewer attractors. The localization domains are then ordered with respect to the ELF critical values yielding bifurcations. Starting at a very low ELF value, we find only one localization domain (the whole space for $\eta(\mathbf{r}) = 0.$) upon increase of the isosurface defining value, we meet a first separation between valence and core domains, at higher ELF values the valence reducible domain is split in its turn. The value of the localization function at the saddle points lying on the separatrix provides a quantitative information to order the basins. The hierarchy of the bifurcation can be visualized by a tree-diagram [36].

2.3.3. *Integrated density over the localization basins*
The partition of the molecular space into basins of attractors allows the calculation of related properties by integration of the property densities over the basins[37]. In particular, for a basin labeled Ω_A, one can define the average population as :

$$\bar{N}(\Omega_A) = \int_{\Omega_A} \rho(\mathbf{r}) d\mathbf{r} \tag{17}$$

Within the framework of our theory, these average populations are referred to as core, di- or polysinaptic and monosynaptic (i.e. lone pair) populations according to the type of attractor which defines the basin. Such average populations over ELF basins have been first calculated by us[36, 38, 39] and recently by Häussermann *et al.* for intermetallic solids[40]. They are not expected to have integral values and the bond populations would be about twice the topologically defined bond orders[41, 42].

The RMS deviation $\sigma(\bar{N}; \Omega_A))$ is defined by[43, 44] :

$$\sigma^2(\bar{N}; \Omega_A)) = \langle N^2 \rangle_{\Omega_A} - \langle N \rangle^2_{\Omega_A} \tag{18}$$

It represents the quantum mechanical uncertainty on $\bar{N}(\Omega_A)$. The variance (or fluctuation) σ^2 has been investigated by Bader in the framework of atomic basins[45]. The variance is expressed in terms of the diagonal elements of the first ($\rho(\mathbf{x})$) and second order ($\pi(\mathbf{x}_1, \mathbf{x}_2)$) density matrices[46] as :

$$\sigma^2(\bar{N}; \Omega) = \int_{\Omega} d\mathbf{x}_1 \int_{\Omega} d\mathbf{x}_2 \pi(\mathbf{x}_1, \mathbf{x}_2) + \bar{N}(\Omega) - [\bar{N}(\Omega)]^2 \tag{19}$$

in which $\mathbf{x}_i$ denotes the space and spin coordinates of the electron labeled i. For a single determinental wavefunction (i.e. Hartree-Fock or Kohn-Sham) $\sigma^2(\bar{N};\Omega)$ is the difference between the basin population and the integral over the basin of the exchange part of the second order density matrix :

$$\sigma^2(\bar{N};\Omega) = \bar{N}(\Omega) - B(\Omega,\Omega) \tag{20}$$

In terms of the orbitals $\phi_i(\mathbf{r})$ and of the occupations n_i^α, n_i^β, $B(\Omega,\Omega)$ is given by :

$$B(\Omega,\Omega) = \sum_i \sum_j (n_i^\alpha n_j^\alpha + n_i^\beta n_j^\beta)\langle\phi_i|\phi_j\rangle_\Omega\langle\phi_j|\phi_i\rangle_\Omega \tag{21}$$

in which

$$\langle\phi_i|\phi_j\rangle_\Omega = \int_\Omega d\mathbf{r}\phi_i^*(\mathbf{r})\phi_j(\mathbf{r}) \tag{22}$$

It is also convenient to define the interbasin integrated exchange density :

$$B(\Omega_A,\Omega_B) = \sum_i \sum_j (n_i^\alpha n_j^\alpha + n_i^\beta n_j^\beta)\langle\phi_i|\phi_j\rangle_{\Omega_A}\langle\phi_j|\phi_i\rangle_{\Omega_B} \tag{23}$$

The fluctuation in a superbasin $\Omega_A \cup \Omega_B$ is :

$$\sigma^2(\bar{N};\Omega_A \cup \Omega_B) = \sigma^2(\bar{N};\Omega_A) + \sigma^2(\bar{N};\Omega_B) - 2B(\Omega_A,\Omega_B) \tag{24}$$

and for the whole space

$$\sigma^2(\bar{N};\Omega_A \cup \Omega_B \cup \ldots) = 0 \tag{25}$$

It follows from eq. 24 that for independent basins σ^2 is an extensive quantity. Following Bader[45], it is useful to introduce the relative fluctuation

$$\lambda(\Omega) = \sigma^2(\bar{N};\Omega)/\bar{N}(\Omega) \tag{26}$$

which is positive and also expected to be less than 1.

3. The Bonding in SiO_2 polymorphs

In crystalline silica the silicon coordination is four for quartz ($P3_221$), tridymite ($F1$ and Cc), cristobalite ($P4_12_12$), coesite ($C2/c$) and keatite ($P4_12_12$), six in stishovite (rutile type structure $P4_2/mnm$) and in the recently high pressure phase with a $CaCl_2$ structure ($Pnnm$) and eight in a fluorite type ($Fm3m$) model structure which is one of the hypothetical post-stishovite modifications investigated by modeling techniques. Of course, the coordination number of oxygen is always half of that of silicon. The conventional discussion of the Si-O bond is focused on the silicon coordination rather than on the oxygen one. Accordingly, in Pauling's representation of the silicon oxygen bond [3], each oxygen donates one electron to the silicon which is then enabled to form at most six single bonds. The silicon has six valence electrons and is essentially of the sp^3d^2 type. In this picture, the ionic character of the bond deduced from the electronegativity rule is 50%. In tetracoordinated polymorphs, each silicon forms two double bonds and two single bonds, the resonance between the limit structures yields a double bond character of about 55% for the Si-O bond. This temptatively explains why the observed bond length is larger than the sum of the covalent raddi and also why the ∠Si-O-Si bond angles observed in low-quartz and low-cristobalite are much more wider than the value expected between single bonds. Though stishovite is not discussed in Pauling paper's, it is worthy to note that this picture accounts for the larger SiO distance observed in this modification.

Another popular description of the chemical bond is provided by the VSEPR model of Gillespie [47, 48]. This model partly explains the geometries of the silica polymorphs investigated here. For Si it cannot give much insight as Si has no lone pairs. The polyhedron with the largest number of staggered bond pairs is preferred for CN 4 (tetrahedron) and CN 6 (octahedron) while for CN 8 the fluorite structure yields a cubic coordination instead of an expected quadratic antiprism. For oxygen the VSEPR model runs into difficulties : for 2-coordinated oxygens, the observed structure is neither consistent with an AX_2E (1 double bond, 1 single bond and 1 lone pair) or AX_2E_2 model (2 single bonds and 2 lone pairs) because the angle $\angle XAX \sim 146°$ is too wide. In stishovite, the three O-Si bonds around the oxygen are coplanar, corresponding to the AX_3E_2 model, but the electron count (4 electron pairs) only allows for an AX_3E model.

Though there is no striking contradiction between the pictures provided by Pauling and by the VSEPR model, the topological approach is expected to give more reliable answers. From the preceeding discussion, it appears that the questions concern more the oxygen side than the silicon one in both Pauling's and VSEPR approaches. The calculation of the wavefunctions have been performed at the all-electron level with the periodic software CRYSTAL92 [49] A polarized split-valence basis set has been used. The valence part is that described by Jolly *et al* [50] whereas the core orbitals are the standard 6-31G ones [51]. The integration over the electron density and ELF function basins has been carried out numerically on a rectangular grid. This technique is less accurate than that designed by Biegler-König *et al* [37]. The estimated error on basin populations is about ten times larger (0.1 e instead of 0.01). However, it is enough accurate to provide reliable

information on the dominant features and on the trends along the series of polymorphs.

3.1. BADER'S ANALYSIS

The values of the oxygen charge $q(O)$, of the laplacian, of the ratio of the perpandicular and parallel components of the hessian matrix and of the bond ellipticity ϵ at the bond critical point are reported in table 2 for the structures investigated here. In Bader's theory a positive value of the laplacian of the density, $\nabla^2\rho(\mathbf{r})$, is a criterion of the closed-shell interaction. Another criterion is ratio $\frac{|\lambda_1|}{\lambda_3}$ which takes larger values (> 1.0) for electron shared interaction than for the closed shell one (< 0.5) and allows a discussion of intermediate cases. The bond ellipticity, $\epsilon = \lambda_1/\lambda_2 - 1$ where λ_1 and λ_2 are the smallest eigenvalues of the hessian matrix, gives an indication of the double bond character. For example, the ellipticity of the C-C bond is respectively 0.0, 0.23 and 0.45 in ethane, benzene and ethylene [16]. The oxygen charges of α-quartz and $CaCl_2$ type structures cannot be accurately computed because technical difficulties (such as hexagonal cell in quartz) downgrade the accuracy of the results. Though the calculated values are rather close to those of α-cristobalite and stishovite, it is not possible to take them into account in reliable comparisons.

TABLE 2. Characterization of atomic interactions in silica polymorphs. All quantities in atomic units. The second entry for stishovite and $CaCl_2$-type structures correspond to the larger Si-O bond. The estimated error on the oxygen charge in quartz amd $CaCl_2$ structure is about $0.2e$.

	$q(O)$	$\nabla^2\rho$	$\frac{\lvert\lambda_1\rvert}{\lambda_3}$	ϵ
α-quartz	-0.7	1.270	0.15	0.015
α-cristobalite	-0.7	1.216	0.16	0.0
stishovite	-1.1	0.652	0.18	0.010
		0.514	0.18	0.0
$CaCl_2$-type	-1.1	1.076	0.16	0.011
		0.918	0.15	0.0
fluorite-type	-1.55	0.326	0.18	0.0

The oxygen net charge increases with the oxygen coordination and the ionic character is $\sim 35\%$ for coordination 2, $\sim 55\%$ for coordination 3 and $\sim$ 75 % for 4. The values provided by the Bader's analysis for quartz and cristobalite are significantly lower those that assumed from electronegativity. In both cases the Laplacian of the density is positive and the $\frac{|\lambda_1|}{\lambda_3}$ ratio very small which corresponds to Bader's closed-shell interaction. This result is not fully consistent with the rather moderate ionic character of the Si-O bond in quartz and cristobalite. However, the links between the sign of the laplacian or the magnitude of the $\frac{|\lambda_1|}{\lambda_3}$ ratio and the interaction type are rather speculative. The bond ellipticity is always negligible and, accordingly, there is no indication for a partial double bond character in quartz and cristobalite.

3.2. TOPOLOGICAL ANALYSIS OF *ELF*

The picture provided by the *ELF* function displays silicon cores and oxygen cores surrounded by a valence shell [52]. The oxygen valence shell as shown on figure 2 contains 3, 5 and 4 basins for the 2, 3 and 4 oxygen coordinations respectively. The pictures for quartz and $CaCl_2$ structures have not been reported because they are almost identical to those of cristobalite and stishovite. There is no additional valence domain on the silicon side, this latter atom only gives rise to a spherical L-shell core domain enclosing the K-shell one.

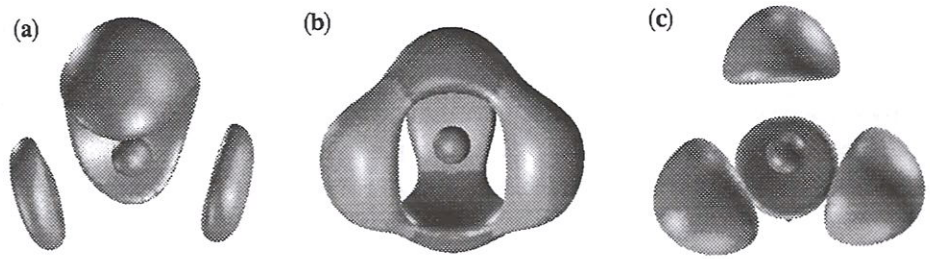

Figure 2. Oxygen $ELF = 0.85$ localization domains of oxygen atoms in (a) cristobalite, (b) stishovite and (c) fluorite-type prototype structure. The bond directions which are not indicated on the figure are along the lines joining the oxygen core domain (the small sphere at the center of the pictures) and the disynaptic domains. In cristobalite the disynaptic domains are the two discs on both side of the core. In stishovite the valence domain is not fully resolved in irreducible domains, the disynpatic attractors are located within the three bulges lying in the horizontal plane. In fluorite-type structure, the four disynaptic domains form a tetrahedron.

In quartz and cristobalite the oxygen atom forms two bonds with the silicons which correspond to the two disynaptic domains on both side of the oxygen core. The oxygen lone pairs give rise to a single monosynaptic basin instead of two as expected from the Lewis structure. This discrepancy from chemical intuition is not an artefact due to the basis set but rather a consequence of the large fluctuation of the electron density within the

valence shell around electronegative atoms. In stishovite, there are three disynaptic basins the attractors of which lie in the plane defined by the nuclei of the silicons bonded to the oxygen and two monosynaptic basins on both sides of this plane. In this case, the $\eta(\mathbf{r}) = 0.85$ isosurface does not achieve the reduction of the valence domain. Finally, the fluorite-type prototype structure is characterized by four disynaptic domains disposed at the vertices of a tetrahedron.

The value of the ELF function at the saddle points between the disynaptic basin and the silicon core is always lower than that between the disynaptic basin of two nearest neighbour oxygens. The difference between such values decreases as the coordination increases. Within a given oxygen valence shell, the ELF value at the saddle point between basins is always close to the attractor value, respectively 0.83 and 0.88 in quartzi for example, indicating a large fluctuation of the electron density between theses basins [36]. This is particularly the case for stishovite and $CaCl_2$-like structures.

The basin population of α-cristobalite, stishovite and fluorite structures are listed in table 3.

TABLE 3. Basin population of oxygen core, disynaptic and monosynaptic attractors.

	core	disynaptic	monosynaptic
α-cristobalite	2.15	1.9	4.0
stishovite	2.15	1.6	1.5
fluorite-type	2.15	1.9_5	

The oxygen core population has been calculated with a fine grid in order to achieve a better accuracy, it is not structure dependent. Though a population of 2 is expected from a Lewis picture, it has been shown by Kohout and Savin that the K-shell population is around $2.2e$ for atoms beyond Ne. [39]. In quartz and cristobalite, there are three valence basins. Two of them are disynaptic with a population slightly less than 2.0, and the remaining is a crescent-shaped monosynaptic basin. It corresponds to the two conventional lone pairs of the Lewis structure and its population is therefore 4.0. In stishovite, each of the three disynaptic basins contains ~ 1.6 electrons whereas a ~ 1.5 electronic population is assigned to each of the monosynaptic ones. In the $CaCl_2$ structure, the monosynaptic basins are dissymmetric because the nuclei of the oxygen and of the three bonded silicons are not in the same plane. As the pyramidization of the OSi_3 fragment is increased, the population of the monosynaptic basin which is on the silicon side is transferred to that on the other side and to the disynaptic

basins. One can expect a structure with three disynaptic basins and one monosynaptic for a large distorsion from the rutile structure. Finally, in the fluorite structure prototype the disynaptic basin populations are ~ 2.0.

In all systems, there is always only one disynaptic attractor with a population ≤ 2 for each Si-O bond. The interaction clearly belongs to the shared disynaptic basin class (electron-shared interaction in Bader's terminology). Moreover, the basin populations indicate single bonds for 2-fold coordinated oxygens rather than a resonance between a single and a double bond as suggested by Pauling. The larger Si-O bond lengths observed in stishovite are explained by the smaller basin population. In the case of the tetracoordinated oxygens, the origin of the lengthening is probably due to the repulsion between nearest neighbour oxygens. In this structure, in spite of a large SiO bond distance (1.918 Å), the oxygen-oxygen distance is much more smaller than in cristobalite (i.e 2.21 Å instead of 2.6 Å).

The location of the disynaptic attractor in the bonding direction provides some information related to the ionic character. In homopolar bonds its position is roughly given by the covalent radii and small deviations may occur due to substituents whereas in heteropolar bonds it is shifted towards the electronegative centre. The monosynaptic attractors are generally closer to the electronegative centre. Distances of attractors from the oxygen nucleus are listed in table 4 together with Bader's bond critical point distances and estimated cationic radii. The distance of the bond critical point to the nucleus defines the atomic radius (in the sense of the covalent radius). In a similar fashion it is possible to define an effective cationic radius as the distance between the nucleus and the core-valence separatrix which is nearly spherical. It is not possible to define an anionic radius in a similar fashion because the envelope of the oxygen valence shell has a rather intricate shape.

TABLE 4. Distances (in Å) of monosynaptic (R_M), disynaptic (R_D) attractors from the oxygen nucleus, atomic (R_A) and cationic radii (R_+) for α-quartz, α-cristobalite, stishovite and fluorite structures.

	quartz	cristobalite	stishovite	fluorite
R_M	0.58	0.58	0.70	
R_D	0.63	0.63	0.69	0.65
R_A(Si)	0.66	0.67	0.67	0.75
R_A(O)	0.94	0.94	1.08	1.17
R_+(Si)	0.60	0.59	0.62	0.64

The valence attractor-nucleus distances increase with the coordination

and decrease as the basin population increases. In stishovite the nucleus-monosynaptic attractor distance is larger than the nucleus-disynatic one, which is probably due to the lower population of the monosynaptic basin with respect to the disynaptic one. The atomic and ionic radii always increase with the coordination. The silicon atomic and ionic radii vary less than the oxygen ones. The increase of the oxygen atomic radius is consistent with the increase of the ionic character of the bond. In high pressure polymorphs, the packing of the oxygen network explains why the SiO_2 units occupy smaller volumes than in quartz and cristobalite in spite of the increase of the atomic radii.

Another interesting feature provided by the ELF analysis is its connection with the VSEPR model. The valence basin is the analogue to the electron domain of Gillespie but with the difference that the former can contain both more than 2 and less than 2 electrons. For instance, in stishovite there are respectively 80% and 75% of a true pair in the disynaptic and monosynaptic domains, whereas in cristobalite even 4 electrons are contained in one monosynaptic basin. In tetracoordinated polymorphs, an AX_2E structure is found around the oxygen atoms. The $\angle SiOSi$ is, however, wider than the value expected by Gillespie for this structure [48] because the monosynaptic basin tends to form a ring around the oxygen core. In molecular prototypes such as $H_3SiOSiH_3$ and $(OH)_3SiOSi(OH)_3$ this angle is always calculated to be greater than 140°. The geometry of stishovite is consistent with AX_3E_2 oxygens in which the electronic domains are partially filled. The transition to the $CaCl_2$ type structure corresponds to a rearrangement towards the local AX_3E type involving an electron transfer from one lone pair domain to the three other domains. Finally, the fluorite-type structure obviously belongs to AX_4.

4. Conclusion

The topological analysis of the density and of the ELF function provides new information to understand the nature of the Si-O bond. On the one hand, the atomic population and the bond ellipticities tell us that the SiO bond is partly ionic and also that there is no evidence for a partial double bond character. This latter point is confirmed by the analysis of the ELF function since there is only one attractor between the oxygen and silicon cores and that its basin population is always less than or equal to 2 electrons. Moreover, it appears more important to consider the oxygen than the silicon to discuss the bonding in silica. The Si-O bond is found to belong to the electron shared interaction by the ELF analysis.

The structural stability of the ELF gradient field warrants the reliability of the qualitative information presented here. In fact, lower quality wavefunctions used in preliminary calculations yield the same number of basins of each type. The noticeable differences which concern the quantitative aspects of this work, i.e. the basin populations, are of the order of magnitude of the error due to the approximate numerical integration. These two errors have the same origin, namely the difficulty of determining precisely the separatrices.

The discussion of the Si-O chemical bond presented in this chapter provides some guidelines to improve interatomic potentials. On the one hand, the analysis of the density gives support to two-body potentials such as those designed by Tsuneyuki [6] and Kramer *al* [7] insofar as the attractors of the valence basins remain rather close to the oxygen centres and because the value of ELF at the saddle points between these basins is rather high. Covalent potential [5] are also successful, because they take into account the mutual repulsion of the valence basins. A trail to improve two-body potentials may be to treat the electrostatic and dispersion interactions as true two-body potentials and to allow more flexibility for the repulsive potential. This can be done by considering that the repulsive interaction occurs between the silicon centre and the core and valence attractors of oxygen. It should be also possible in this way to model the variation in the number of valence attractors occurring with a change of the oxygen coordination.

References

1. Pauling, L. (1939) *The nature of the chemical bond,* Cornell University Press, Ithaca, NY.
2. Pauling, L. (1952) Interatomic distances and bond character in the oxygen acids and related substances, *J. Phys. Chem.,* **56,** 361-365.
3. Pauling, L. (1980) The nature of silicon-oxygen bonds. *Am. Mineralogist,* **65,** 321-323.
4. Gibbs, G. V., Downs, J. W. and Boisen, Jr. M. B. (1994) The elusive SiO bond. *Rev. Mineral.,* **29,** 331-368.
5. Lasaga, A. C., and Gibbs, G. V. (1987) Application of Quantum Mechanical Potential Surfaces to Mineral Physics Calculations. *Phys. Chem. Minerals,* **14,** 107-117.
6. Tsuneyuki, S., Matsui, Y., Tsukada, M., and Aoki, H. (1988) First-Principles Interatomic Potential of Silica Applied to Molecular Dynamics, *Phys. Rev. Lett.,* **61,** 869-872.
7. Kramer, G.J., Farragher, N.P., van Beest, B.W.H., and van Santen, R.A. (1991) Interatomic Force Fileds for Silicas, Alluminophosphates, and zeolites: Derivation Based on Ab Initio Calculations, *Phys. Rev.,* **B43,** 5068-5080.
8. Kassab, E., Seiti, K. and Allavena, M. (1991) Theoretical Determination of Relative Acidity in Zeolite (Faujasite). *J. Phys. Chem.,* **95,** 9425-9431.
9. Allavena, M. and Kassab, E. (1993) Molecular interactions in solid state and quantum chemistry : A model problem, the proton transfer in zeolites. *Solid State Ionics,* **61,** 33-39.
10. Sauer, J. (1994) Structure and reactivity of zeolite catalysts Atomistic modeling usin ab initio techniques, in J. Weitkamp et al (eds.), *Zeolithes and Related Microporous materials : State of the Art, Studies in Surface Science and Catalysis, vol. 84,* Elsevier, Amsterdam, pp. 2039-2057.

11. Gibbs, G. V., Meagher, E. P., Newton, M. D., and Swanson, D. K. (1981) A comparison of experimental and theoretical bond length and angle variations for minerals, inorganic solids, and molecules, in M. O'Keefe and A. Navrotsky (eds.), *Structure and Bonding in Crystals*, Academic Press, New York, Vol. 1 pp. 195-225.
12. Silvi, B., D'Arco, Ph., Saunders, V. R., and Dovesi, R. (1991) Periodic Hartree-Fock study of Minerals: Tetracoordinated Silica Polymorphs. *Phys. Chem. Minerals*, **17**, 674-680.
13. Silvi, B., D'Arco, Ph., and Causá, M. (1990) Periodic Pseudo-potential Hartree-Fock Study of α-quartz structure SiO_2 and GeO_2. *J. Chem. Phys.*, **93**, 7225-7230.
14. Silvi, B., Allavena, M., Hannachi, Y., and D'Arco, Ph. (1992) Pseudopotential periodic Hartree-Fock study of the cristobalite phases of SiO_2 and GeO_2. *J. Am. Ceram. Soc.*, **75**, 1239-1246.
15. Bachrach, S. M. (1994) Population analysis and Electron Densities from Quantum Mechanics. in K. B. Lipkowwitz and D. B. Boyd (eds.), *Computational Chemistry*, VCH, New York, Vol. 5. pp. 171-227.
16. Bader, R. F. W. (1990) *Atoms in molecules*, Oxford Science Publications, Oxford.
17. Silvi, B. and Savin, A. (1994) Classification of chemical bonds based on topological analysis of electron localization function. *Nature*, **371**, 683-686.
18. Becke, A., and Edgecombe, K. E. (1990) A simple measure of electron localization in atomic and molecular systems. *J. Chem. Phys.*, **92**, 5397-5403.
19. Thom, R. (1972) *Stabilité Structurelle et Morphogénèse*. Intereditions, Paris.
20. Ruedenberg, K. (1962) The Physical Nature of the Chemical Bond. *Rev. Mod. Phys.*, **34**, 326-376.
21. Shewell, J. R. (1959) On the Formation of Quantum-Mechanical Operators. *Am, J. Phys.*, **27**, 16-21.
22. Cohen, L. (1966) Generalized Phase-Space Distribution Functions. *J. Math. Phys.*, **7**, 781-786.
23. Dahl, J. P. (1982) The Wigner Function. *Physica*, **114A**, 439-444.
24. Dirac, P. A. M. (1958) *The Principles of Quantum Mechanics*, Oxford University Press, Oxford.
25. Cohen, L. (1979) Local kinetic energy in quantum mechanics. *J. Chem. Phys.*, **70**, 788-789.
26. von Weizsäcker, C. F. (1935) Zur Theorie der Kernmassen. *Z. Phys.*, **96**, 431-458.
27. Tal, Y., and Bader, R. F. W. (1978) Studies of the Energy Density Functional Approach. I. Kinetic Energy. *Int. J. Quant. Chem.*, **S12**, 153-168.
28. Sears, S. B., Parr, R. G., and Dinur, U. (1980) On the Quantum-Mechanical Kinetic Energy as a Measure of the Information in a Distribution. *Israel J. Chem.*, **19**, 165-173.
29. Gázquez, J. L., and Ludeña, E. V. (1981) The Weizsacker term in Density Functional Theory. *Chem. Phys. Lett.*, **83**, 145-148.
30. Ludeña, E. V. (1982) On the nature of the correction to the Weizsacker term. *J. Chem. Phys.*, **76**, 3157-3160.
31. Kohn, W. and Sham, L. J. (1965) Self-Consistent Equations Including Exchange and Correlation Effects. *Phys. Rev.*, **140**, 1133-1138.
32. Savin, A., Jepsen, O., Flad, J., Andersen, O. K., Preuss, H., and von Schnerring, H. G. (1992) *Angew. Chem. Int. Ed. Engl.*, **31**, 323-324.
33. Lacks, D. J., and Gordon, R. G. (1994) Tests of nonlocal kinetic energy functionals. *J. Chem. Phys.*, **100**, 4446-4452.
34. Lee, H., Lee, C., and Parr, R. G. (1991) Conjoint gradient correction to the Hartree-Fock kinetic-and exchange-energy density functionals. *Phys. Rev.*, **A44**, 768-771.
35. Yang, W. (1986) Gradient correcttion in Thomas-Fermi theory. *Phys. Rev.*, **A34**, 4575-4585.
36. Savin, A., Silvi, B. and Colonna, F. (1996) Topological analysis of the electron localization function applied to delocalized bonds. *Can. J. Chem.*, **74**, 1088-1096.
37. Biegler-König, F. W., Bader, R. F. W., and tang, T. H. (1982) Calculation of the Average properties of Atoms in Molecules. II. *J. Comput. Chem.*, **3**, 317-328.
38. Savin, A. (1993) Electron Localization Function (ELF) in molecules and solids. *Second International Conference on Inorganic Chemistry*, Stuttgart, Germany.
39. Kohout, M., and Savin, A. (1996) Influence of the core-valence separation on the Electron Localization Function. *Int. J. Quant. Chem.* (in press)
40. Häussermann, U., Wengert, S. and Nesper, R. (1994) Unequivocal Partitioning of Crystal Structures, Exemplified by Intermetallic Phases Containing Aluminium. *Angew. Chem. Int. Ed. Engl.*, **33**, 2073-2076.
41. Cioslowski, J. and Mixon, S. T. (1991) Covalent Bond Orders in the Topological Theory of Atoms in Molecules. *J. Am. Chem. Soc.*, **113**, 4142-4145.
42. Ángyán, J. G., Loos, M. and Mayer, I. (1994) Covalent Bond Orders and Atomic Valence Indices in the Topological Theory of Atoms in Molecules. *J. Phys. Chem.*, **98**, 5244-5248.
43. Messiah, A. (1962) *Mécanique Quantique, Tome I.*, Dunod, Paris, p. 113.
44. Claverie, P. and Diner, S. (1976) Statistical and Stochastic Aspects of the Delocalization Problem in Quantum Mechanics. in O. Chalvet, R. Daudel, S. Diner and J. P. Malrieu (eds.) *Localization and Delocalization in Quantum Chemistry*, Reidel Publishing Company, Dordrecht, Vol. 2 pp. 395-448.
45. Bader, R. F. W. (1975) Comparison of Loge and Virial Methpds of Partitioning Molecular Charge Distributions. in O. Chalvet, R. Daudel, S. Diner and J. P. Malrieu (eds.) *Localization and Delocalization in Quantum Chemistry*, Reidel Publishing Company, Dordrecht, Vol. 1 pp. 15-38.
46. McWeeny, R. (1989) *Methods of Molecular quantum Mechanics*, Academic Press, London, pp. 119-124.
47. Gillespie, R. G. (1972) *Molecular Geometry*, Van Nostrand Reinhold, London.
48. Gillespie, R. G., and Robinson, E. A. (1996) Electron Domains and the VSEPR Model of Molecular Geometry. *Angew. Chem. Int. Ed. Engl.*, **35**, 495-514.
49. Dovesi, R., Saunders, V. R., and Roetti, C. (1992) *CRYSTAL 92, an ab-initio Hartree-Fock LCAO program for periodic systems*, Theoretical Chemistry Group, University of Turin and SERC Daresbury Laboratory.
50. Jolly, L-H., Silvi, B., and D'Arco, Ph. (1994) Periodic Hartree-Fock study of minerals : Hexacoordinated SiO_2 and GeO_2 polymorphs. *Eur. J. Mineral.*, **6**, 7-16.
51. Hehre, W. J., Ditchfield, R., and Pople, J. A. (1972) Self-consistent molecular-orbital methods. XII. Further extensions of gaussian-type basis sets for use in molecular orbital studies of organic molecules. *J. Chem. Phys.*, **38**, 2257-2261.
52. Pepke, E., Murray, J., and Hwu, T.-Z. (1993) *SciAn*, Supercomputer Computations Research Institute, Florida State University, Tallahassee, Florida.